Sci. Rep. Kanazawa Univ.
Vol. 59, pp. 27–50, 2015

Numerical methods for 1-D hyperbolic-type problems with free boundary

Faizal MAKHRUS*, Yoshiho AKAGAWA, Alvi SYAHRINI

Graduate School of Natural Science and Technology,
Kanazawa University, Kakuma, Kanazawa, 920–1192, Japan

(Received June 29, 2015 and accepted in revised form August 31, 2015)

Abstract We study a 1-D hyperbolic-type problem with free boundary which describes the motion of a piece of tape being peeled off from a surface. The graph of the solution represents the shape of the tape, which displays contact angle dynamics at the free boundary (the location of peeling). The contact angle dynamics lead to singularities located on the free boundary, which cause a slight difficulty. Under some assumptions, this problem can be solved numerically by a so-called fixed domain method. This method is a numerical method which transforms the domain of the positive part of the solution into a fixed domain using a change of variables and solves the problem in that domain. Although this method has a high accuracy, it can not be applied in some cases. Hence other numerical methods are chosen for solving a regularized problem, i.e., the singularities on the free boundary are regularized by a smoothing function. The numerical methods are: two types of finite difference methods, the finite element method and discrete Morse flow. In this paper, the error of solving the regularized problem instead of the original problem is calculated. Since the choice of the parameter for smoothing function is important for the accuracy, we propose a formula to estimate the optimal parameter in order to minimize the error. This formula is verified by numerical experiments and we find that it can estimate the optimal parameter. In addition, based on comparisons between the numerical methods, we find that the finite difference methods have better performance than the other methods.

Keywords. hyperbolic free boundary problem, fixed domain method, finite element method, discrete Morse flow

1 Introduction

In this paper we investigate numerical methods for solving a one-dimensional hyperbolic-type problem with a free boundary. Our problem can be derived from a physical

*Corresponding author. Current address: Department of Computer Science, Faculty of Mathematics and Natural Sciences, Gadjah Mada University, Sekip Unit 3, Bulaksumur, Sleman, Indonesia.
e-mail: faizal_makhrus@yahoo.com

model of a piece of tape which is attached to a surface and peeled off from the edge smoothly. Under certain assumptions [2], the motion of the tape is described by a stationary point of the following action integral in a suitable function space:

$$J(u) = \int_0^\tau \int_\Omega \left(\frac{1}{2}|\nabla u|^2 - \frac{1}{2}(u_t)^2 \chi_{u>0} + \frac{Q^2}{2}\chi_{u>0} \right) dxdt, \tag{1.1}$$

where $u\colon (0,\tau)\times\Omega \mapsto \mathbf{R}$ is a scalar function which represents the shape of the tape, Ω is a domain in $\mathbf{R}^d (d \geq 1)$, Q is the surface tension and $\chi_{u>0}$ is a characteristic function of the set $\{(x,t) : u(x,t) > 0\}$. The following Euler-Lagrange equation can be derived from functional (1.1) under certain assumptions [2]:

$$\begin{cases} u_{tt} = \Delta u & \text{in } (\Omega \times (0,\tau)) \cap \{u > 0\}, \\ |\nabla u|^2 - (u_t)^2 = Q^2 & \text{on } (\Omega \times (0,\tau)) \cap \partial\{u > 0\}. \end{cases} \tag{1.2}$$

When $d = 1$, under certain conditions, [3] showed that the existence and the uniqueness of its solutions are obtained locally.

On the other hand, we derive the following equation from (1.2) (see Section 2):

$$\chi_{\overline{\{u>0\}}} u_{tt} = \Delta u - \frac{Q^2}{|Du|}\mathscr{H}^d \lfloor \partial\{u > 0\} \quad \text{in } \Omega \times (0,\tau), \tag{1.3}$$

where $\mathscr{H}^d$ is the d-dimensional Hausdroff measure and $Du = \left(\dfrac{\partial u}{\partial x_1}, \ldots, \dfrac{\partial u}{\partial x_d}, \dfrac{\partial u}{\partial t} \right)$. Next, we consider the following equation as the regularized problem of (1.3)

$$\chi_{\{u>0\}} u_{tt} = \Delta u - \frac{Q^2}{2}(\chi^\varepsilon)'(u) \quad \text{in } \Omega \times (0,\tau), \tag{1.4}$$

where $\chi^\varepsilon(u) \in C^\infty(\mathbf{R})$ is a smoothing of the characteristic function such that $(\chi^\varepsilon)' \geq 0$ and

$$\chi^\varepsilon(u) = \begin{cases} 0 & u \leq 0, \\ 1 & u \geq \varepsilon. \end{cases}$$

The main purpose of this paper is to investigate the error obtained in solving (1.4) utilizing several numerical methods. The error is obtained by comparing with the solution of (1.2) which is equivalent to the original problem (1.3) if the solution is non-negative. We solve (1.2) by the fixed domain method. This method has high accuracy [2]. Therefore we use its solution to calculate the error, and from this error, we know that the choice of parameter ε is important to the accuracy. Therefore we propose a formula to get the optimal ε and confirm that this formula applies based on our experiments. We discuss this in Section 4.1–4.2.

The numerical methods that we use are:

1. explicit method 1 (spatial central difference + time forward difference)

2. explicit method 2 (spatial and time central difference)
3. finite element method (FEM)
4. discrete Morse flow (DMF).

We choose explicit method 1 and 2 as they are standard methods. Here, explicit method 2 is a standard finite difference method which can be used to analyze the error of the solution of the regularized problem. We choose FEM as it is widely used to approximate solutions of hyperbolic problems and DMF is chosen since it is used in many hyperbolic-type problems with constraints [1]. We conduct the comparisons of these numerical methods in Section 4.4.

The second purpose of this paper is to investigate the effectivity of different kinds of smoothed characteristic functions. We consider two types of smoothed characteristic functions and compare them to get the suitable one (see Section 4.3). The last purpose is to implement more advanced case such as a model in which there are more than one free boundary points that appear or vanish during the simulation (see Section 4.5).

2 Derivation of (1.3)

This section depends on [4]. We show the derivation of (1.3). Let $Q_T := \Omega \times (0,\tau)$. We assume $u \in H^2(\{u>0\}) \cap C(Q_T)$ is a nonnegative solution of (1.2) such that contact set $\{u>0\}$ has a sufficiently regular boundary and $\{u>0\} \subset C^{0,1}$. By definition

$$(u_{tt} - \Delta u)(\varphi) = -\int_{Q_T} \{u_t \varphi_t - \nabla u \cdot \nabla \varphi\} dxdt,$$

where $u_{tt} - \Delta u$ is a measure. Since u is nonnegative,

$$\begin{aligned}\left(\chi_{\overline{\{u>0\}}} u_{tt}\right)(E) &= \int_{E \cap \overline{\{u>0\}}} u_{tt} \\ &= u_{tt}\left(E \cap \overline{\{u>0\}}\right) \\ &= u_{tt}(E),\end{aligned}$$

where $E \subset Q_T$. Thus $\chi_{\overline{\{u>0\}}} u_{tt} = u_{tt}$ in the measure sense. Then, by using the above assumptions, we can calculate

$$\begin{aligned}\left(\chi_{\overline{\{u>0\}}} u_{tt} - \Delta u\right)(\varphi) &= -\int_{Q_T} \{u_t \varphi_t - \nabla u \cdot \nabla \varphi\} dxdt \\ &= \int_{\{u>0\}} (u_{tt} - \Delta u)\varphi dxdt - \int_{\partial\{u>0\}} \frac{|\nabla u|^2 - (u_t)^2}{|Du|} \varphi d\mathscr{H}^m \\ &= -\int_{\partial\{u>0\}} \frac{Q^2}{|Du|} \varphi d\mathscr{H}^m,\end{aligned}$$

and directly obtain (1.3).

3 Numerical Methods

From this section throughout this paper, we assume that Ω is 1-dimensional. This section explains our numerical methods. Let us introduce some notations. The domain Ω is divided into N intervals, $x_0 < x_1 < \cdots < x_N$, then the characteristic function is smoothed as follows

$$(\chi^\varepsilon)'(u) = \begin{cases} 1/\varepsilon & 0 < u < \varepsilon, \\ 0 & \text{otherwise.} \end{cases} \tag{3.1}$$

As we will show later in Section 4.3, the smoothness of χ^ε does not significantly influence accuracy, and therefore to speed up the numerical computations we use a smoothing function χ^ε as above that is only Lipschitz continuous. Next, the characteristic function is

$$\chi_{\{u>0\}}(x_i,t) = \begin{cases} 1 \text{ if } \max\left(u(x_{i-1},t),u(x_i,t),u(x_{i+1},t)\right) > 0, \\ 0 \text{ otherwise} \end{cases}$$

and

$$\chi^\varepsilon(u) = \int_0^u (\chi^\varepsilon)'(s)ds.$$

At last, since we are interested in observing the biggest error of the solutions during time t, we define the error of numerical solutions as

$$E_u = \max_{\substack{i=0,\ldots,N \\ k=0,\ldots,M}} |u^*(x_i,t_k) - u_i^k|,$$

where u^* is the exact solution or fixed domain method solution and u_i^k is the numerical solution at x_i in time t_k.

3.1 Fixed domain method (FDM)

For equation (1.2), we build the numerical solution as explained in [2]. We assume that the free boundary contains a single point $l(t)$. Here, $u(x,t)$ is the solution at position x and time t, $l(t)$ is the position of the boundary at time t and $l_0 = l(0)$. Since the key of fixed domain method in this case is to solve only in $\{u > 0\}$, the coordinates are mapped using function

$$y = \frac{2x}{l(t)} - 1$$

and become $(0,l(t)) \times (0,\tau) \ni (x,t) \mapsto (y,t) \in (-1,1) \times (0,\tau)$. Rewriting equation (1.2) using (y,t), one has

$$u_{tt} - \frac{4 - ((y+1)l'(t))^2}{l(t)^2} u_{yy} - 2(y+1)\frac{l'(t)}{l(t)} u_{ty} - (y+1)\frac{l(t)l''(t) - 2(l'(t))^2}{l(t)^2} u_y = 0$$

in $(-1,1)\times(0,\tau)$ and

$$l'(t) = \pm\sqrt{1-\left(\frac{Ql(t)}{2u_y(1,t)}\right)^2},$$

where $l'(t) \geq 0$. Now, the y-space $[-1,1]$ is discretized into $\tilde{N}$ equal intervals and we can get the following equations

$$\frac{d}{dt}u^i(t) = v^i(t), \tag{3.2}$$

$$\begin{aligned}\frac{d}{dt}v^i(t) = {} & \frac{4-((y_i+1)l'(t))^2}{l(t)^2}\frac{u^{i+1}(t)-2u^i(t)+u^{i-1}(t)}{(\Delta y)^2} \\ & + 2(y_i+1)\frac{l'(t)}{l(t)}\frac{v^{i+1}(t)-v^{i-1}(t)}{2\Delta y} \\ & + (y_i+1)\frac{l(t)l''(t)-2(l'(t))^2}{l(t)^2}\frac{u^{i+1}(t)-u^{i-1}(t)}{2\Delta y}, \quad i=1,\ldots,\tilde{N}-1,\end{aligned} \tag{3.3}$$

$$l'(t) = \pm\sqrt{1-\left(\frac{Ql(t)}{2u_y^N(t)}\right)^2}. \tag{3.4}$$

We solve (3.2)–(3.4) using the 4^{th}-order Runge-Kutta method.

3.2 Explicit method 1 (spatial central difference and time forward difference)

We represent equation (1.4) using an explicit method with u_{xx} approximated by central differencing. Suppose $u_t = v$ then

$$\frac{d}{dt}u_i(t) = v_i(t), \tag{3.5}$$

$$\frac{d}{dt}v_i(t) = \frac{u_{i-1}(t)-2u_i(t)+u_{i+1}(t)}{(\Delta x)^2} - \frac{Q^2}{2}(\chi^\varepsilon)'(u_i(t)), \quad \text{if } \chi_{\{u>0\}}(x_i,t)=1, \tag{3.6}$$

$$v_i(t) = 0, \quad \text{if } \chi_{\{u>0\}}(x_i,t)=0, \tag{3.7}$$

where $i=1,\ldots,N-1$. We solve (3.5)–(3.7) using the 4^{th} order Runge-Kutta.

3.3 Explicit method 2 (spatial and time central difference)

This method utilizes a standard finite difference discretization. We approximate u_{xx} and u_{tt} from equation (1.4) using centered differencing. Here, $[0,\tau]$ is divided into M equal intervals, $0 = t_0 < t_1 < \cdots < t_M = \tau$, so we have

$$\chi_{\{u>0\}}(x_i,t_k)\frac{u_i^{k+1}-2u_i^k+u_i^{k-1}}{(\Delta t)^2} = \frac{u_{i+1}^k-2u_i^k+u_{i-1}^k}{(\Delta x)^2} - \frac{Q^2}{2}(\chi^\varepsilon)'(u_i^k),$$
$$i=1,\ldots,N-1 \text{ and } k=1,\ldots,M-1,$$

where $u_i^k = u(x_i, t_k)$. Then we calculate the solutions using the following

$$\begin{cases} u_i^{k+1} = 2u_i^k - u_i^{k-1} \\ \qquad\quad +(\Delta t)^2 \left(\dfrac{u_{i+1}^k - 2u_i^k + u_{i-1}^k}{(\Delta x)^2} - \dfrac{Q^2}{2}(\chi^\varepsilon)'(u_i^k) \right), & \text{if } \chi_{\{u>0\}}(x_i,t_k) = 1, \\ u_i^{k+1} = 0, & \text{if } \chi_{\{u>0\}}(x_i,t_k) = 0. \end{cases} \quad (3.8)$$

3.4 Finite Element Method

To implement finite element method, we multiply equation (1.4) by any test function $\xi \in C_0^\infty(\Omega)$ and integrate over the space domain

$$\int_\Omega (\chi_{\{u>0\}} u_{tt} - u_{xx} + \frac{Q^2}{2}(\chi^\varepsilon)'(u))\xi dx = 0.$$

By integration by parts we obtain

$$\int_\Omega (\chi_{\{u>0\}} u_{tt}\xi + u_x\xi_x + \frac{Q^2}{2}(\chi^\varepsilon)'(u)\xi)dx = 0, \quad \forall \xi \in C_0^\infty(\Omega). \quad (3.9)$$

We divide Ω into N intervals and find the approximate solution of (3.9) in the set

$$V_t = \{u \in C^0(\bar{\Omega}) : \ u|_{\partial\Omega} = f(\cdot,t),\ u \text{ is linear on every } [x_{k-1}, x_k],\ k = 1, \ldots, N\}$$

for each time $t \in (0,\tau)$, where $f : \bar{\Omega} \times [0,\tau]$ is a given function. Then the approximate solution can be described by $u(x,t) = \sum_{i=0}^N a_i(t)\varphi_i(x)$, where

$$\varphi_i(x) = \left(1 - \frac{|x - x_i|}{\Delta x}\right)_+, \quad i = 0, \ldots, N.$$

Here the symbol $(\ )_+$ implies $(f(x))_+ = \max(f(x), 0)$. We substitute the approximate solution u to (3.9)

$$\int_\Omega \left(\chi_{\{u>0\}} \sum_{i=0}^N a_i'' \varphi_i \xi + \sum_{i=0}^N a_i \varphi_i' \xi' + \frac{Q^2}{2}(\chi^\varepsilon)' \sum_{i=0}^N a_i \varphi_i \xi \right) dx = r, \ \forall \xi \in C_0^\infty(\Omega), \quad (3.10)$$

where r is the residual which comes from the approximated representation of function u. We choose φ_j, $j = 1, \ldots, N-1$, as our test function and rewrite (3.10) as follows:

$$\sum_{i=0}^N \left[a_i'' \int_\Omega \chi_{\{u>0\}} \varphi_i \varphi_j dx \right] + \sum_{i=0}^N \left[a_i \int_\Omega \varphi_i' \varphi_j' dx \right] + \frac{Q^2}{2} \int_\Omega (\chi^\varepsilon)' \sum_{i=0}^N a_i \varphi_i \varphi_j dx = 0,$$
$$\text{j = 1,2,...,N-1.}$$

This can be written in a vector form

$$Ba'' + Aa + \frac{Q^2}{2} C(a) = p,$$

where a is the column vector with entries $a_1, \ldots, a_{N-1}$,

$$A = \frac{1}{\Delta x}\begin{bmatrix} 2 & -1 & 0 & 0 & 0 & \cdots & 0 & 0 \\ -1 & 2 & -1 & 0 & 0 & \cdots & 0 & 0 \\ 0 & -1 & 2 & -1 & 0 & \cdots & 0 & 0 \\ \vdots & \vdots & \vdots & \vdots & \vdots & \vdots & \ddots & \vdots \\ 0 & 0 & 0 & 0 & 0 & \cdots & -1 & 2 \end{bmatrix}$$

and

$$B = \frac{\Delta x}{6}\begin{bmatrix} 4\tilde{\chi}(a_1) & \tilde{\chi}(a_1) & 0 & 0 & 0 & \cdots & 0 & 0 \\ \tilde{\chi}(a_2) & 4\tilde{\chi}(a_2) & \tilde{\chi}(a_2) & 0 & 0 & \cdots & 0 & 0 \\ 0 & \tilde{\chi}(a_3) & 4\tilde{\chi}(a_3) & \tilde{\chi}(a_3) & 0 & \cdots & 0 & 0 \\ \vdots & \vdots & \vdots & \vdots & \vdots & \vdots & \ddots & \vdots \\ 0 & 0 & 0 & 0 & 0 & \cdots & \tilde{\chi}(a_{N-1}) & 4\tilde{\chi}(a_{N-1}) \end{bmatrix}.$$

Here, $\tilde{\chi}(a_i) = 1$, whenever $\max(a_{i-1}, a_i, a_{i+1})$ is greater than zero and $\tilde{\chi}(a_i) = 0$ otherwise. Here, C is a column vector whose elements are determined by a and p is determined by boundary values.

We approximate a'' using central difference with $a_i^k = a_i(t_k)$ and $a^k = (a_1^k, \ldots, a_{N-1}^k)$:

$$B\frac{a^{k+1} - 2a^k + a^{k-1}}{(\Delta t)^2} + Aa^k + \frac{Q^2}{2}C(a^k) = p.$$

The final form is

$$Ba^{k+1} = 2Ba^k - Ba^{k-1} - (\Delta t)^2\left(Aa^k + \frac{Q^2}{2}C(a^k) - p\right). \tag{3.11}$$

We define $a_i^{k+1} = 0$, if $b_{ii} = 0$ where b_{ii} is the diagonal element of matrix B at i^{th} row. In general, matrix B is non-symmetric. We can change the position of the known value of a_i^{k+1} to the right hand side and adjust the matrix B to be a symmetric matrix. Now, we approximate the solution a^{k+1} of (3.11) by conjugate gradient method.

3.5 Discrete Morse Flow

Let us consider problem (1.4) with u^0 as the initial value, v^0 as the initial velocity and $u^1 = u^0 + \Delta t v^0$. Now, we determine the time step $\Delta t = \tau/M$, where $M > 0$ is a natural number. Then, the approximate solution for the next time $t = k\Delta t$, $k = 2, 3, \ldots, M$ is defined by the minimizer $u^k \in \mathscr{K}$ of

$$J_k(u) = \int_\Omega \frac{|u - 2u^{k-1} + u^{k-2}|^2}{2(\Delta t)^2}\chi_{\{u>0\}}dx + \frac{1}{2}\int_\Omega |\nabla u|^2 dx + \frac{Q^2}{2}\int_\Omega \chi^\varepsilon(u)dx,$$

where $u^j(x)=u(x,t_j)$, $t_j=j\Delta t$ $(j=k-2,k-1)$ and $\mathscr{K}=\{u\in \mathbf{W}^{1,2}(\Omega);u=g \text{ on } \partial\Omega\}$.

We approximate u^k as a piecewise linear function, so that the functional's values are approximated:

$$J_k(u)\approx\sum_{i=1}^{N}\int_{x_{i-1}}^{x_i}\left(\frac{|u-2u^{k-1}+u^{k-2}|^2}{2(\Delta t)^2}\chi_{\{u>0\}}+\frac{1}{2}|\nabla u|^2+\frac{Q^2}{2}\chi^{\varepsilon}(u)\right)dx. \tag{3.12}$$

We calculate the first term as follows:

$$\int_{x_{i-1}}^{x_i}\frac{|u-2u^{k-1}+u^{k-2}|^2}{2(\Delta t)^2}\chi_{\{u>0\}}dx$$
$$=\begin{cases}(v^2+w^2+vw)\dfrac{\Delta x}{6(\Delta t)^2} & u_{i-1}>0,\ u_i>0,\\ (w^2+(v_2)^2+wv_2)\dfrac{x_c-x_i}{6(\Delta t)^2} & u_{i-1}\le 0,\ u_i>0,\\ ((w_2)^2+v^2+w_2v)\dfrac{x_c-x_{i-1}}{6(\Delta t)^2} & u_{i-1}>0,\ u_i\le 0,\\ 0 & \text{otherwise,}\end{cases}$$

where $v=|u_{i-1}-2u_{i-1}^{k-1}+u_{i-1}^{k-2}|$, $w=|u_i-2u_i^{k-1}+u_i^{k-2}|$, $u_{i-1}=u(x_{i-1},t)$, $u_i=u(x_i,t)$, $v_2=v-\dfrac{w-v}{u_i-u_{i-1}}u_{i-1}$, $w_2=v_2$ and $x_c=x_{i-1}-\dfrac{\Delta x}{u_i-u_{i-1}}u_{i-1}$. The second term is

$$\frac{1}{2}\int_{x_{i-1}}^{x_i}|\nabla u_i|^2dx=\frac{(u_{i+1}-u_i)^2}{2\Delta x},$$

and for the third term we have

$$\int_{x_{i-1}}^{x_i}\chi^{\varepsilon}(u)dx$$
$$=\begin{cases}\Delta x & u_{\max}\ge\varepsilon,\ u_{\min}\ge\varepsilon,\\ 1-\dfrac{\Delta x}{u_{\min}-u_{\max}}\left(\dfrac{-u_{\min}(u_{\min}-\varepsilon)}{2\varepsilon}-(\varepsilon-u_{\max})\right) & u_{\max}\ge\varepsilon,\ 0\le u_{\min}<\varepsilon,\\ \dfrac{u_{\max}\Delta x}{2(u_{\max}-u_{\min})} & u_{\max}\ge\varepsilon,\ u_{\min}\le 0,\\ \dfrac{\Delta x}{2\varepsilon}(u_{\max}+u_{\min}) & 0\le u_{\max}<\varepsilon,\ 0\le u_{\min}<\varepsilon,\\ \dfrac{u_{\max}^2\Delta x}{2\varepsilon(u_{\max}-u_{\min})} & 0\le u_{\max}<\varepsilon,\ u_{\min}\le 0,\\ 0 & \text{otherwise,}\end{cases}$$

where $u_{\max}=\max(u_{i-1},u_i)$ and $u_{\min}=\min(u_{i-1},u_i)$. We find the minimizer of (3.12) using a non-linear conjugate gradient method.

4 Numerical results

In this section, we explain our experiments and the results. In our experiments we compare two problems. The first problem is

$$\begin{cases} u_{tt} = u_{xx} & \text{in } (\Omega \times (0,\tau)) \cap \{u > 0\}, \\ (u_x)^2 - (u_t)^2 = Q^2 & \text{on } (\Omega \times (0,\tau)) \cap \partial\{u > 0\}, \\ u(0,t) = f(t), \\ u(x,0) = g(x), \\ u_t(x,0) = h(x), \end{cases}$$

approximated by the fixed domain method and the second problem is

$$\begin{cases} \chi_{\{u>0\}} u_{tt} = u_{xx} - \dfrac{Q^2}{2}(\chi^\varepsilon)'(u) & \text{in } \Omega \times (0,\tau), \\ u(0,t) = f(t), \\ u(x,0) = g(x), \\ u_t(x,0) = h(x), \end{cases}$$

approximated by two types of finite different method, FEM or DMF. The initial conditions of our experiments are

$$\begin{aligned} l_0 &= \frac{1}{\sqrt{Q^2 + f'(0)^2}}, \\ g(x) &= \max(1 - \frac{1}{l_0}x, 0), \\ h(x) &= \begin{cases} f'(0) & 0 < x \le l_0, \\ 0 & l_0 < x, \end{cases} \end{aligned}$$

and $f(t)$ are as follows:

Case 1 Peeling speed is constant $f(t) = at + 1$. The exact solution of this case is $u(x,t) = \max(1 + t - \frac{1}{l_0}x, 0)$.

Case 2 Peeling speed is increasing $f(t) = (at+1)^2$.

Case 3 Peeling speed is decreasing $f(t) = \sqrt{at+1}$.

Case 4 Peeling speed is stopping at some times $f(t) = 1 + at + \sin t$

Case 5 Peeling direction is downward (pasting the tape).

$$\begin{aligned} g(x) &= \max(10 - \frac{1}{l_0}x, 0), \\ f(t) &= 10 - at, \\ h(x) &= \begin{cases} f'(0) & 0 < x \le l_0, \\ 0 & l_0 < x. \end{cases} \end{aligned}$$

Case 6 Peeling directions are upward and downward (oscillating tape) $f(t) = 1 + 0.3\sin t$.

In addition, we construct the exact solution of (1.4) for a special case. Let $\Omega = \mathbf{R}$, then we describe problem (1.4) as

$$\chi_{\{u>0\}} u_{tt} = \Delta u - \frac{Q^2}{2}(\chi^\varepsilon)'(u) \quad \text{in } \mathbf{R}\times(0,\tau). \tag{4.1}$$

Let $u^\varepsilon : (0,\tau)\times\mathbf{R} \mapsto \mathbf{R}$ be the exact solution of (4.1) and we assume that u^ε is written as

$$u^\varepsilon(x,t) = F(z), \quad z = x - vt,$$

where v is a constant and $0 < v < 1$, $F : \mathbf{R} \to \mathbf{R}$; $F(0) = 0$, $F'(0) = 0$, $F \in C^{1,1}(\mathbf{R})$. This solution can be considered as peeling tape with constant peeling speed, where the solution is increasing but keeps its shape. Therefore we get

$$\chi_{\{F>0\}} v^2 F''(z) = F''(z) - \frac{Q^2}{2}(\chi^\varepsilon)'(F). \tag{4.2}$$

We separate F into three intervals $\{F \geq \varepsilon\}$, $\{0 < F < \varepsilon\}$ and $\{F = 0\}$. We assume that the free boundary point is at $z = 0$ $(F(0) = 0)$ and $z = z_\varepsilon$ $(F(z_\varepsilon) = \varepsilon)$ as shown in Figure 1. Then we can construct the exact solution as follows

$$F(z) = \begin{cases} -\dfrac{Q}{\sqrt{1-v^2}}(z - z_\varepsilon) + \varepsilon & z < z_\varepsilon, \\ \dfrac{Q^2}{4\varepsilon(1-v^2)} z^2 & z_\varepsilon \leq z < 0, \\ 0, & 0 \leq z. \end{cases} \tag{4.3}$$

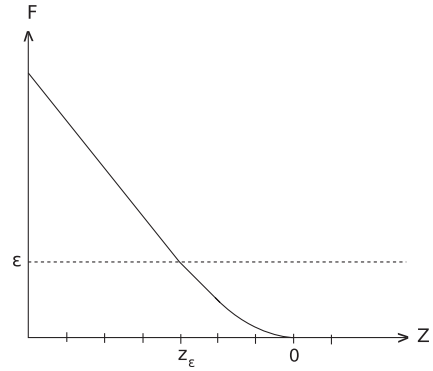

Figure 1: Exact solution (4.2)

4.1 Error in the peeling tape model using smoothed characteristic functions

We solve cases 1–6 using explicit method 2 and compare with the exact solution for case 1 and the fixed domain method solutions for cases 2–6. The parameters are shown in Table 1 below.

Table 1: Parameters for explicit method 2 and fixed domain method

	Q^2	Ω	a	Δt	Δx
explicit method 2	1	$[0,15]$	1	$0.9\Delta x$	varied
fixed domain method	1	$[-1,1]$	1	0.0005625	0.002

The comparisons are shown in Figure 2. From the figures, we can see that the errors of solutions for all cases tend to be small when Δx is decreasing with ε. They show that small and big ε give large error and so we analyze this error pattern. Since the precise error is difficult to find, we only approximate it. Here, the error of the explicit method 2 satisfies the inequality

$$\max_{\substack{i=0,\dots,N\\k=0,\dots,M}} |u^*(x_i,t_k)-u_i^k| \le E_1+E_2,$$

where

$$E_1=\max_{\substack{i=0,\dots,N\\k=0,\dots,M}} |u^*(x_i,t_k)-u^\varepsilon(x_i,t_k)|, \qquad E_2=\max_{\substack{i=0,\dots,N\\k=0,\dots,M}} |u^\varepsilon(x_i,t_k)-u_i^k|$$

and u^* is the exact solution of problem (1.2), u^ε is the exact solution of (1.4) and u is the solution of (3.8). From this inequality we expect to obtain the error pattern.

We calculate the error of finite difference (explicit method 2). We define

$$e_i^k=\frac{u^\varepsilon(x_i,t_{k-1})-2u^\varepsilon(x_i,t_k)+u^\varepsilon(x_i,t_{k+1})}{\Delta t^2}-\frac{u^\varepsilon(x_{i-1},t_k)-2u^\varepsilon(x_i,t_k)+u^\varepsilon(x_{i+1},t_k)}{\Delta x^2}$$
$$+\frac{Q^2}{2}(\chi^\varepsilon)'(u^\varepsilon(x_i,t_k)) \tag{4.4}$$

and subtract (4.4) from (4.1) to obtain

$$u_{tt}^\varepsilon-u_{xx}^\varepsilon+\frac{Q^2}{2}(\chi^\varepsilon)'(u^\varepsilon)=\frac{u^\varepsilon(x_i,t_{k-1})-2u^\varepsilon(x_i,t_k)+u^\varepsilon(x_i,t_{k+1})}{\Delta t^2}$$
$$-\frac{u^\varepsilon(x_{i-1},t_k)-2u^\varepsilon(x_i,t_k)+u^\varepsilon(x_{i+1},t_k)}{\Delta x^2}+\frac{Q^2}{2}(\chi^\varepsilon)'(u^\varepsilon(x_i,t_k))-e_i^k.$$

Since the error occurs near $z=0$ and z_ε, at first we calculate for $z=0$ $(x_i-vt_k=0)$.

$$e_i^k=\frac{F(v\Delta t)-2F(0)+F(-v\Delta t)}{\Delta t^2}-u_{tt}-\frac{F(-\Delta x)-2F(0)+F(\Delta x)}{\Delta x^2}+u_{xx}.$$

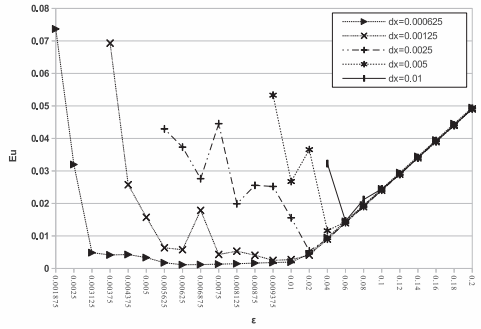

(a) E_u at time $\tau = 9$ in case 1

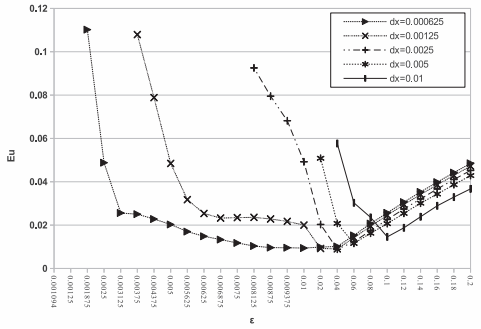

(b) E_u at time $\tau = 9$ in case 2

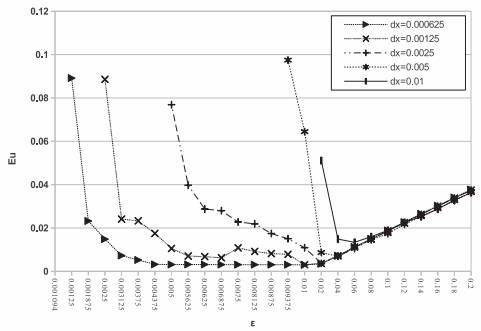

(c) E_u at time $\tau = 9$ in case 3

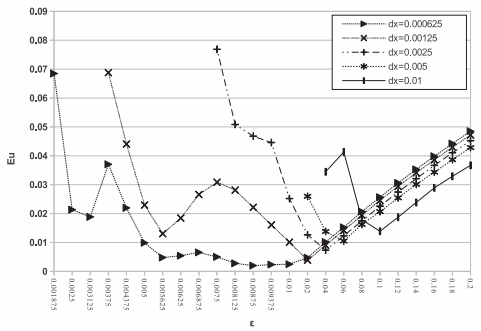

(d) E_u at time $\tau = 9$ in case 4

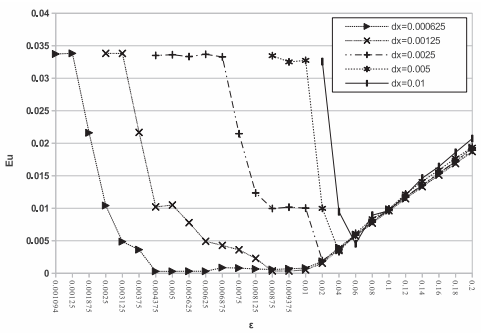

(e) E_u at time $\tau = 9$ in case 5

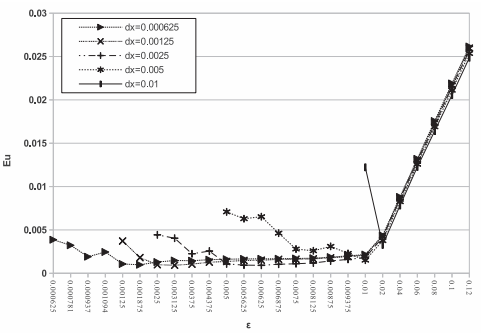

(f) E_u at time $\tau = 7$ in case 6

Figure 2: The errors of explicit method 2 for cases 1–6

Since we want to find the upper bound of the error, we note

$$\begin{aligned}\left|e_i^k\right| &\le \left|\frac{F(v\Delta t)-2F(0)+F(-v\Delta t)}{\Delta t^2}-u_{tt}\right|+\left|-\frac{F(-\Delta x)-2F(0)+F(\Delta x)}{\Delta x^2}+u_{xx}\right| \\ &\le \left|\frac{-Q^2v^2}{4\varepsilon(1-v^2)}\right|+\left|\frac{Q^2}{4\varepsilon(1-v^2)}\right|.\end{aligned}$$

Since $0 < v < 1$, we have

$$\left|e_i^k\right| \leq \frac{Q^2}{2\varepsilon(1-v^2)}.$$

In the same way, we can get the estimate of $\left|e_i^k\right|$ for z_ε, which is also less than or equal to $\dfrac{Q^2}{2\varepsilon(1-v^2)}$. Since $|e_i^k|$ is the error of the finite differencing, we expect

$$E_2 \sim \frac{g_u^2 \Delta x}{2\varepsilon}, \tag{4.5}$$

where g_u is the norm of the gradient of the solution and $g_u^2 = \dfrac{Q^2}{1-v^2}$. In this experiment, we can consider the gradient is a constant C.

Next, we assume the error $E_1 = \tilde{C}\varepsilon$. Therefore the total error is

$$\max_{i=0,\ldots,N} |u^*(x_i,t_k) - u_i^k| \leq \tilde{C}\varepsilon + \frac{C\Delta x}{\varepsilon}. \tag{4.6}$$

The graph of this total error can be seen in Figure 3. In this figure, there are two Δx:

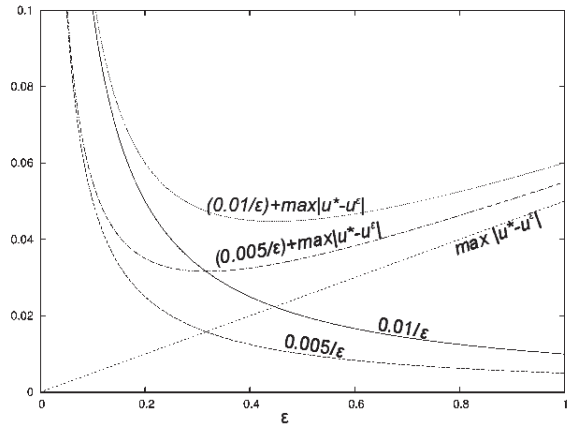

Figure 3: Estimation from above of the total error for explicit method 2

0.01 and 0.005. When Δx decreases, the error also decreases for particular ε. It also shows that when ε is big or small, the error increases. This is approximately similar to the error pattern in Figure 2a and serves to justify our results.

4.2 Comparisons of solution having different gradient

We are also interested in investigating the choice of ε to get optimal error related to the gradient of the solution near the free boundary point (g_u). The relation between g_u and the error is shown in (4.5). The gradient of the solution is approximated by calculating

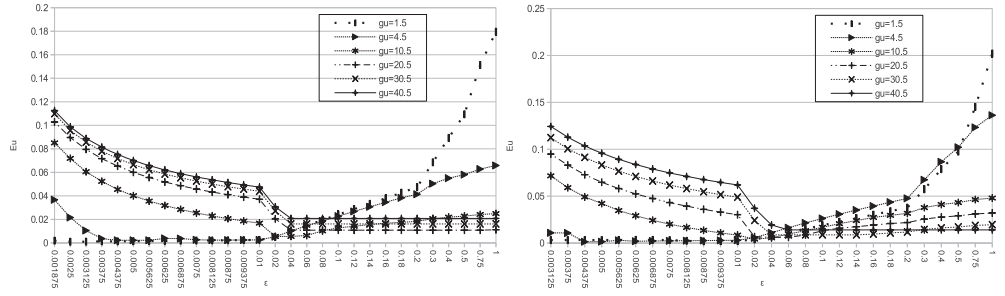

(a) case 1 (b) case 2

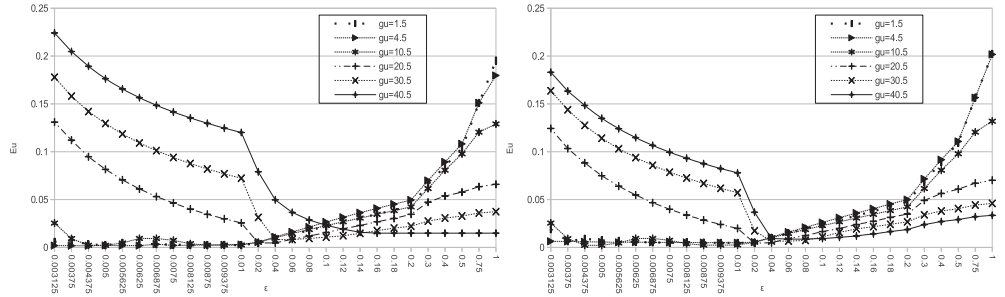

(c) case 3 (d) case 4

Figure 4: The errors of solution for case 1–4 with different gradient and $\Delta x = 0.000625$ at $\tau = 7$

the linear regression of five u_i whose values are nearest to the value 0.1. This value is chosen since, based on Figure 2a–2d, when $\varepsilon = 0.1$, they display similar errors for different Δx.

To see the relation between the error of the solutions and g_u, we conduct a few experiments using cases 1–4 with different g_u. We choose only cases 1–4 since they are enough to represent different kinds of solutions. We set the gradient of the solution at time $\tau = 7$ to be 1 to 40. The results are shown in Figures 4 and 5. Figure 4 shows that the range of optimal ε becomes larger when g_u increases. In addition, Figure 5 shows that there are two surfaces. The lower surfaces describe the lower bound of the range for the optimal ε, while the upper surfaces describe the upper bound of the range for the optimal ε. From the figure, the range of the optimal ε becomes large if the gradient of the solution increases.

The optimal ε can be derived from (4.6). Therefore we have

$$\varepsilon = C g_u \sqrt{\Delta x}. \tag{4.7}$$

From the experiments above, the range of constant C in (4.7) is shown in Figure 6. In this figure, each vertical line indicates the range of constant C which applies for the gradient 1 to 40. It shows when the constant C is between 0.15–0.16, it satisfies for all

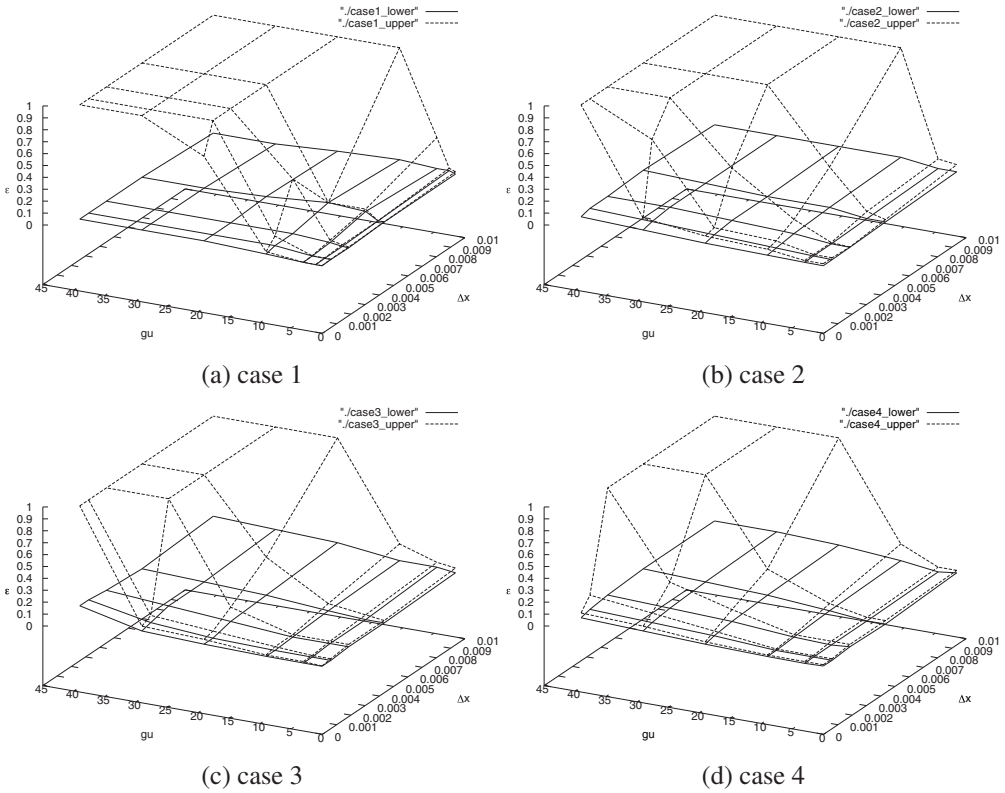

(a) case 1 (b) case 2

(c) case 3 (d) case 4

Figure 5: The lower and upper bound of optimal ε for cases 1–4 at $\tau = 7$

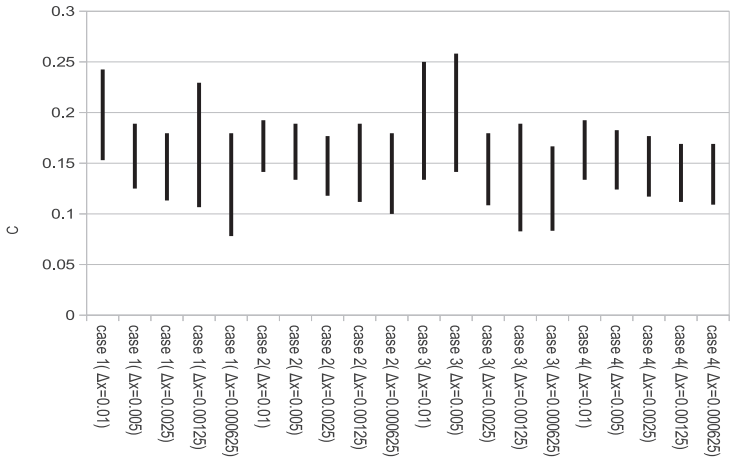

Figure 6: The range of constant C for cases 1–4 with different Δx

cases and Δx. Therefore, we conclude that the constant C is approximately 0.15–0.16.

4.3 Comparisons of smoothed characteristic functions

Here, we will compare two smoothed characteristic functions satisfying (3.1) and

$$(\chi^{\varepsilon})'(u) = \begin{cases} \dfrac{hu}{a} & 0 < u < a, \\ h & a \le u \le \varepsilon - a, \\ \dfrac{h(\varepsilon - u)}{a} & \varepsilon - a \le u \le \varepsilon, \\ 0 & \text{otherwise}, \end{cases} \tag{4.8}$$

where

$$a = \frac{\varepsilon}{b}, \qquad h = \frac{1}{\varepsilon - a},$$

b is a positive number. Function (4.8) has smoother transitions than (3.1). We want to know whether smooth transitions influence the accuracy. The goal of this experiment is to get the appropriate smoothed characteristic function.

We apply these two functions in equation (1.4) with parameters $Q^2 = 1$, $\Omega = [0, 15]$, $a = 1$, $\Delta x = 0.005$ and $\Delta t = 0.9\Delta x$ and solve using explicit method 2. The errors for each case at time level $\tau = 9$ (case 6 uses $\tau = 7$) are shown in Figure 7. The errors are calculated using

$$\tilde{E}_u = \max_{\substack{i=0,\ldots,N \\ k=0,\ldots,M}} |u^*(x_i, t_k) - (u^{(3.1)})_i^k| \quad \text{or} \quad \tilde{E}_u = \max_{\substack{i=0,\ldots,N \\ k=0,\ldots,M}} |u^*(x_i, t_k) - (u^{(4.8)})_i^k(t)|,$$

where $(u^{(3.1)})_i^k$ and $(u^{(4.8)})_i^k$ are solutions with smoothed characteristic function (3.1) and (4.8) respectively. From Figure 7, we see that the error difference between (3.1)

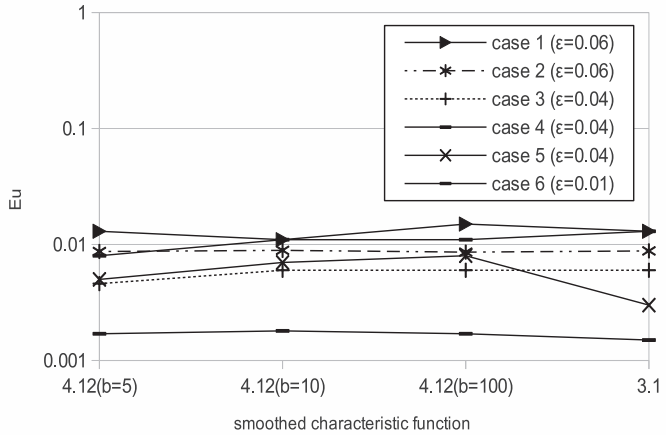

Figure 7: Comparison of smoothed characteristic functions

and (4.8) are slightly different, with an order of $10^{-3} - 10^{-4}$. Therefore, (3.1) is an adequate smoothed characteristic function.

4.4 Comparisons of numerical methods

To compare numerical methods, we conduct two experiments. The first experiment is to numerically solve (4.2) and compare the results with the exact solution (4.3). In order to do this, we consider a case similar to case 1 with initial conditions

$$u^{\varepsilon}(x,0) = \begin{cases} -\dfrac{1}{l_0}x + 1 & 0 \le x \le l_0 - \varepsilon l_0, \\ \dfrac{(x - l_0 - \varepsilon l_0)^2}{4\varepsilon (l_0)^2} & l_0 - \varepsilon l_0 \le x \le l_0 + \varepsilon l_0, \\ 0 & l_0 + \varepsilon l_0 \le x, \end{cases}$$

$$u^{\varepsilon}(0,t) = \sqrt{\frac{1}{(l_0)^2} - Q^2}\, t + 1,$$

$$u_t^{\varepsilon}(x,0) = \begin{cases} \sqrt{\dfrac{1}{(l_0)^2} - Q^2} & 0 \le x \le l_0 - \varepsilon l_0, \\ \dfrac{\sqrt{\dfrac{1}{(l_0)^2} - Q^2}}{2\varepsilon l_0}(x - l_0 - \varepsilon l_0) & l_0 - \varepsilon l_0 \le x \le l_0 + \varepsilon l_0, \\ 0 & l_0 + \varepsilon l_0 \le x. \end{cases}$$

The exact solution is $u^{\varepsilon}(x,t) = F(x - l_0 - (\varepsilon/a) - \sqrt{1 - (Q/a)^2}\, t)$. We choose the parameters $Q^2 = 1,\ \Omega = [0,15],\ \Delta x = 0.005$ and Δt as in Table 2 below.

Table 2: Δt for numerical methods

explicit method 1	explicit method 2	FEM	DMF
0.0045	0.0045	0.0025	0.0005

The error is calculated by

$$C_u = \max_{\substack{i=0,\ldots,N \\ k=0,\ldots,M}} |u^{\varepsilon}(x_i,t_k) - u_i^k|,$$

and Figure 8 shows the error results. In Figure 8, the errors C_u of all methods decreases as ε increases and explicit method 2 has both the lowest and the biggest errors.

The second experiment applies the numerical methods to cases 1–6 and compares the errors of each method. We choose the parameters $Q^2 = 1,\ \Omega = [0,15],\ \Delta x =$

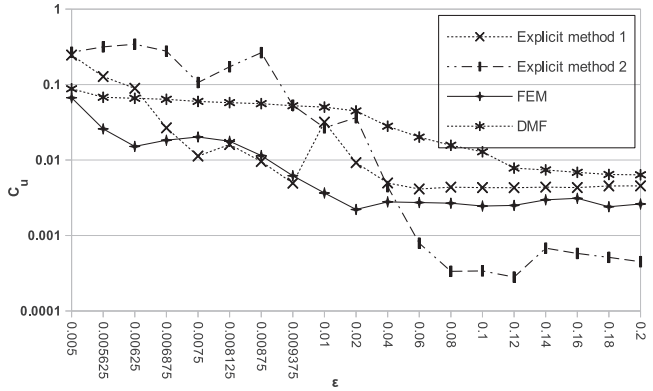

Figure 8: Error of numerical methods and exact solution of equation (4.2)

Table 3: E_u at time $\tau = 9$ (cases 1–5) and $\tau = 7$ (case 6)

case	explicit method 1	explicit method 2	FEM	DMF
1	0.008	0.011	0.01	0.0097
2	0.02	0.02	0.023	0.012
3	0.0079	0.006	0.0075	0.0074
4	0.013	0.013	0.014	0.0097
5	0.005	0.003	0.005	0.006
6	0.007	0.008	0.007	0.009

Table 4: Computation time

	fixed domain method	explicit method 1	explicit method 2	FEM	DMF
time	2s	3s	3s	6s	$>$ 15mins

0.005, $\varepsilon = 0.04$ and Δt as in Table 2. The errors of the methods are shown in Table 3 and the computation time of each method can be seen in Table 4.

The error differences of each numerical method in Table 3 are relatively small (order $10^{-3} - 10^{-4}$). Therefore, we conclude that all methods have similar accuracy. However, based on the computation time in Table 4, DMF has a large computation time due to its algorithm and small Δt. We try several Δt for DMF and find that when $\Delta t = 1/10\Delta x$ the error corresponding to the DMF solution approach the errors of the other methods. Regarding the FEM approach, we find that $\Delta t \leq 1/2\Delta x$ gives stable solutions.

4.5 Advanced cases

We also test more intricate cases where the free boundary points are more than one and they appear or vanish during time t. We choose $\Omega = [0,2]$ (except case 7) , $Q^2 = 1$, $\Delta x = 0.005$, Δt as shown in Table 2 and initial conditions are listed below.

case 7 peeling tape from two sides

We modify case 1 above by peeling off from the beginning and end of the tape. Our domain is $\Omega = [0,5]$. The peeling velocities at both sides are the same as case 1. The tape is peeled off until the free boundaries vanish and from here it becomes a wave equation. Since case 1 has an exact solution, it can be used to obtain the exact solution of the wave equation using d'Alembert's formula. In this case, we only consider the exact solution in the middle point of Ω.

To get the exact solution of the wave equation at $x = 2.5$, we first consider the exact solution of case 1,

$$g(x,t) = \max(1 + t - \frac{1}{l_0}x, 0)$$

and its velocity $h(x,t)$. The time that the free boundary disappears is $t = 2.535$. From this time on, the solution evolves by the wave equation: we define $t_{wave} = t - 2.535$ and the exact solution is

$$\begin{aligned} u^*(2.5, t_{wave}) =& 0.5 \Bigg(g(2.5 + t_{wave}, 2.535) + g(2.5 - t_{wave}, 2.535) \\ &+ \int_{2.5-t_{wave}}^{2.5+t_{wave}} h(2.5, 2.535) dx \Bigg). \end{aligned} \tag{4.9}$$

case 8 pulling down a string from the middle

$$u(x,0) = 0.5,\ u_t(x,0) = -20x(2-x),\ u(0,t) = u(2,t) = 0.5$$

case 9 an unstable curve

$$u(x,0) = \max(-0.8(2x-2)^6 + 2(2x-2)^4 - 2.2(2x-2)^2 + 1, 0)$$

$$u_t(x,0) = 0,\ u(0,t) = u(2,t) = 0$$

case 10 collision of four waves

$$u(x,t) = \sum_{i=1}^{4} \max(-6(x - a_i - t)^2 + 0.16, 0),$$

where $a_i = a_{i-1} + 0.37$ and $a_0 = 6$.

The numerical solutions corresponding to the above cases are shown in Figures 9–12.

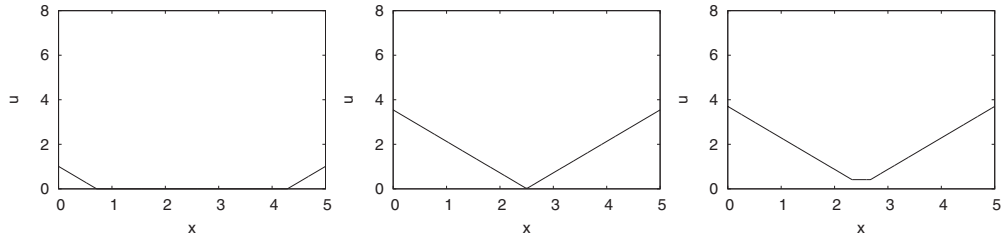

(a) $t = 0$ (b) $t = 2.825$ (c) $t = 3$

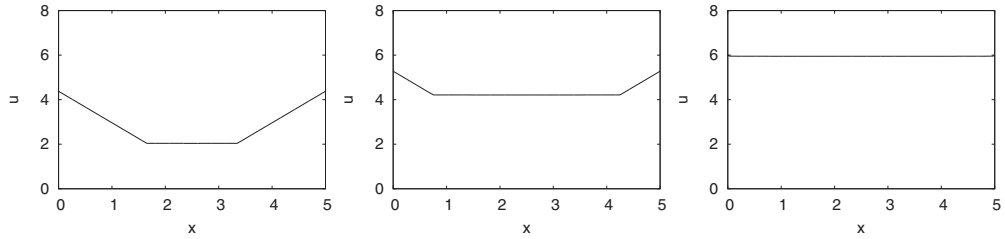

(d) $t = 3.75$ (e) $t = 4.75$ (f) $t = 5$

Figure 9: The numerical solutions of case 7

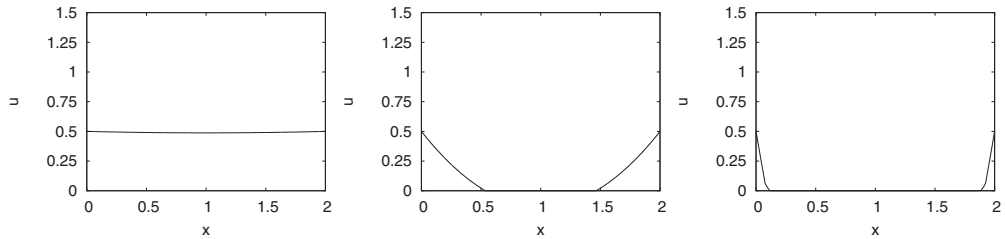

(a) $t = 0$ (b) $t = 0.016$ (c) $t = 0.032$

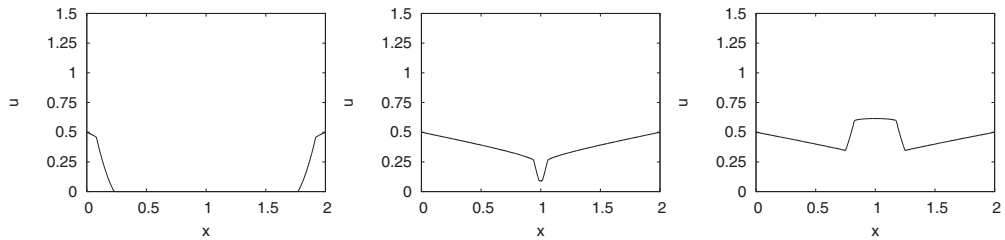

(d) $t = 0.16$ (e) $t = 1.17$ (f) $t = 1.4$

Figure 10: The numerical solutions of case 8

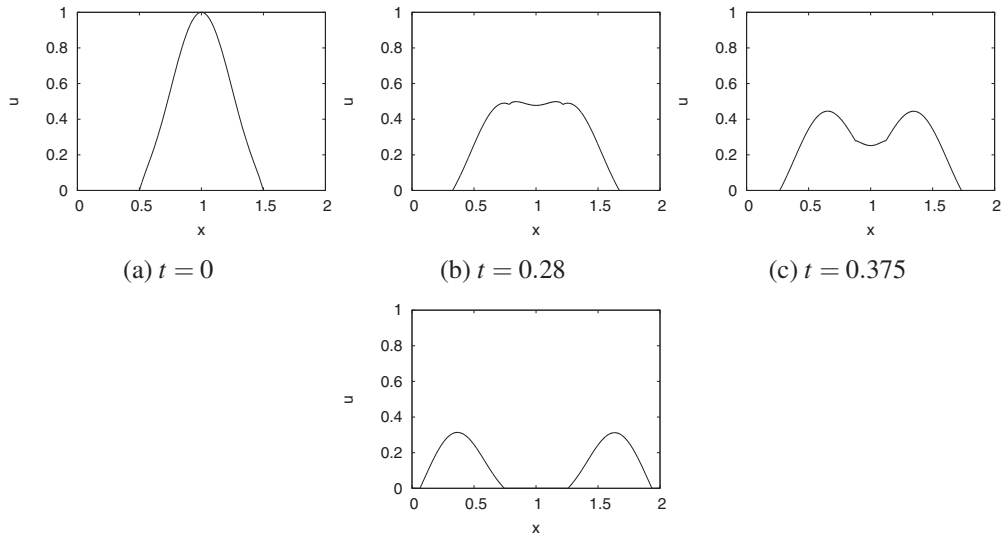

(a) $t = 0$ (b) $t = 0.28$ (c) $t = 0.375$

(d) $t = 0.65$

Figure 11: The numerical solutions of case 9

For case 7, we compare the solution $u(2.5,t)$ at the mid point when the free boundaries vanish with the exact solution (4.9) and calculate

$$E = |u^*(2.5,t) - u(2.5,t)|.$$

We choose $\varepsilon = 0.04$. The results can be seen in Figure 13. The error is of the same order as the error of case 1 (see 2a).

For cases 8–10, as we do not have the exact solutions, we calculate the differences between explicit method 1, FEM or DMF and explicit method 2. We calculate the difference by

$$D_u = \max_{\substack{i=0,\ldots,N \\ k=0,\ldots,M}} |(u^{ex2})_i^k - u_i^k|,$$

where u^{ex2} is the solution of explicit method 2 and u is the solution of explicit method 1, FEM or DMF. The comparison is shown in Table 5, from which we see that the differences of the solutions are of the order 10^{-3}. Hence we can say that all methods are relatively similar.

Table 5: D_u of numerical methods

case	t	explicit method 1	FEM	DMF
7	0.2	0.0023	0.0008	0.0038
8	0.6	0.0061	0.0014	0.0017
9	0.5	0.0032	0.0016	0.0025

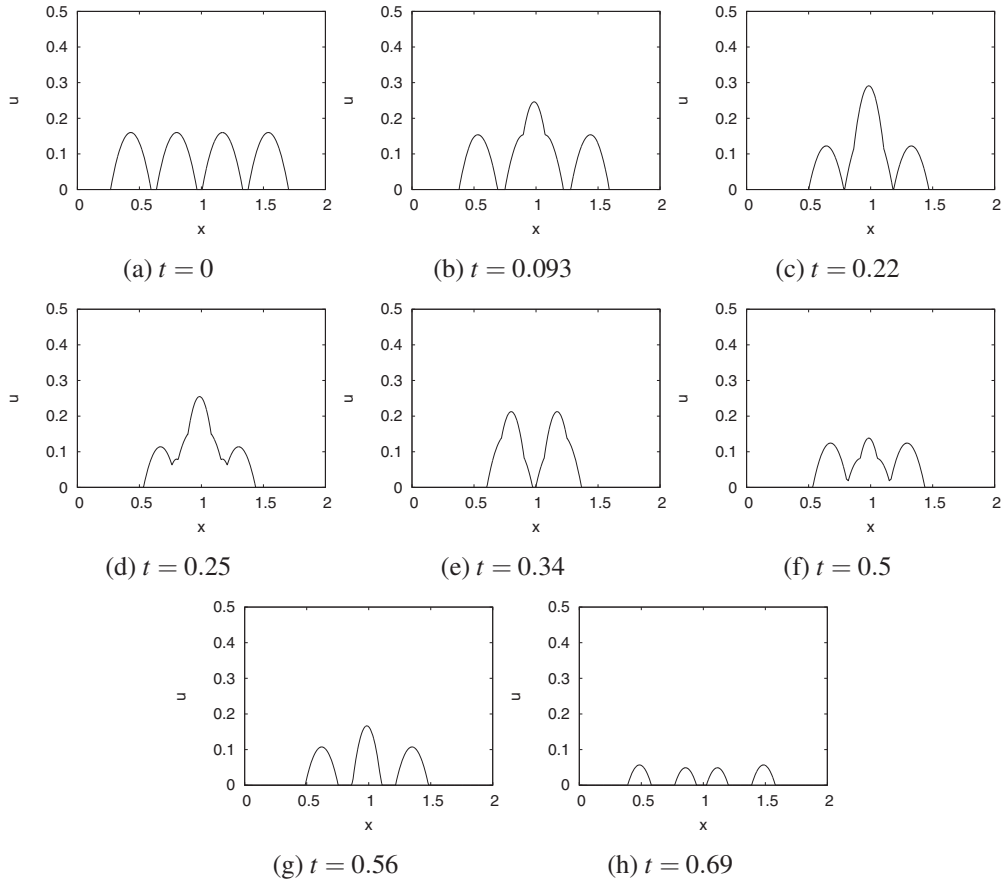

(a) $t = 0$ (b) $t = 0.093$ (c) $t = 0.22$

(d) $t = 0.25$ (e) $t = 0.34$ (f) $t = 0.5$

(g) $t = 0.56$ (h) $t = 0.69$

Figure 12: The numerical solutions of case 10

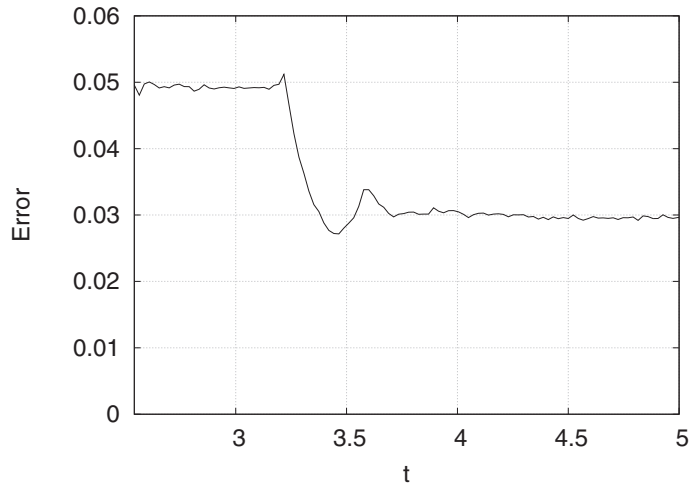

Figure 13: Error in case 7 at $u(2.5,5)$

We summarize the features of the numerical methods in Table 6 below.

Table 6: The features of numerical methods

	Fixed domain method	Explicit method 1	Explicit method 2	FEM	DMF
accuracy	10^{-11}	10^{-3}	10^{-3}	10^{-3}	10^{-3}
stability	$\Delta t \leq 0.1\Delta x$	$\Delta t = 0.9\Delta x$	$\Delta t = 0.9\Delta x$	$\Delta t \leq 0.5\Delta x$	$\Delta t \leq 0.1\Delta x$
easiness of implementation	medium	medium	easy	medium	hard
computation time	fast	fast	fast	fast	slow
(dis-)appearance of free boundary	no	yes	yes	yes	yes

From the table we conclude: first, the accuracy of fixed domain method is the highest compared to the other methods. Second, DMF requires small Δt (at least $\leq 0.1\Delta x$) for stability and it makes this method slow. Third, the computation time of DMF is long since the minimization process needs many iterations. Fourth, only fixed domain method can not handle the appearance and disappearance of the free boundary point.

5 Conclusion

We solved a one dimensional hyperbolic-type problem with free boundary and a smoothed characteristic function by the finite difference method (explicit method 2) and compared the solution with exact or fixed domain method solutions. From experiments 1 and 2, we obtained the error pattern of explicit method 2 and confirmed using approximation that this error pattern holds. The observed pattern shows that there is an optimal ε which minimizes the error. Therefore we proposed formula (4.7) to calculate the optimal ε with respect to the gradient of the solution and Δx. This formula includes a constant which, based on our experiments, we found to be within 0.15 to 0.16 for gradients with values between 1 and 40. In experiment 3, we conclude that smooth transitions in the smoothed characteristic function do not significantly influence the accuracy of the method and that (3.1) is an adequate smoothed characteristic function. In experiments 4 and 5, we compared four numerical methods solving the peeling tape problem with more involved initial and boundary data and found that explicit methods 1 and 2 have good performance.

Acknowledgement

The authors express their gratitude to Professor Seiro Omata and Professor Katsuyoshi Ohara for introducing this problem and several ideas.

References

[1] E. GINDER, K. SVADLENKA, *A variational approach to a constrained hyperbolic free boundary problem,* Nonlinear Analysis **71** (2009) 1527–1537

[2] H. IMAI, K. KIKUCHI, K. NAKANE, S. OMATA, T. TACHIKAWA, *A numerical approach to the Asymptotic Behavior of Solution of a one-dimensional free boundary problem of hyperbolic type,* Japan J. of Ind. and Appl. Math. **18** (2001), 43–58.

[3] K. KIKUCHI, S. OMATA, *A free boundary problem for a one dimensional hyperbolic equation,* Adv. Math. Sci. Appl. **9** (1999), 775–786

[4] S. OMATA, N. POZAR, *Private discussion,* 2014.